

Spectroscopic study of low-temperature hydrogen absorption in palladium

K. Ienaga, H. Takata, Y. Onishi, Y. Inagaki, H. Tsujii, T. Kimura, and T. Kawae

Citation: [Applied Physics Letters](#) **106**, 021605 (2015); doi: 10.1063/1.4905729

View online: <http://dx.doi.org/10.1063/1.4905729>

View Table of Contents: <http://scitation.aip.org/content/aip/journal/apl/106/2?ver=pdfcov>

Published by the [AIP Publishing](#)

Articles you may be interested in

[Novel insight into the hydrogen absorption mechanism at the Pd\(110\) surface](#)

J. Chem. Phys. **140**, 134705 (2014); 10.1063/1.4869544

[Inelastic electron tunneling spectroscopy study of ultrathin Al₂O₃ – TiO₂ dielectric stack on Si](#)

Appl. Phys. Lett. **97**, 202905 (2010); 10.1063/1.3518478

[Imaging and vibrational spectroscopy of single pyridine molecules on Ag\(110\) using a low-temperature scanning tunneling microscope](#)

J. Chem. Phys. **124**, 204708 (2006); 10.1063/1.2200350

[Superconductivity of nanometer-size Pb islands studied by low-temperature scanning tunneling microscopy](#)

Appl. Phys. Lett. **88**, 113115 (2006); 10.1063/1.2184758

[Low-temperature dynamics and spectroscopy in exohedral rare-gas C₆₀ fullerene complexes](#)

J. Chem. Phys. **114**, 5156 (2001); 10.1063/1.1350918

A promotional banner for Applied Physics Reviews. On the left is a thumbnail of a journal cover titled 'AIP Applied Physics Reviews' featuring a diagram of a layered structure. The main text reads 'NEW Special Topic Sections' in large white letters. Below this, it says 'NOW ONLINE' in yellow, followed by 'Lithium Niobate Properties and Applications: Reviews of Emerging Trends' in white. The AIP Applied Physics Reviews logo is in the bottom right corner.

NEW Special Topic Sections

NOW ONLINE
Lithium Niobate Properties and Applications:
Reviews of Emerging Trends

AIP Applied Physics
Reviews

Spectroscopic study of low-temperature hydrogen absorption in palladium

K. Ienaga,^{1,a)} H. Takata,¹ Y. Onishi,¹ Y. Inagaki,¹ H. Tsujii,² T. Kimura,³ and T. Kawae¹

¹Department of Applied Quantum Physics, Faculty of Engineering, Kyushu University, Motoooka, Nishi-Ku, Fukuoka 819-0395, Japan

²Department of Physics, Faculty of Education, Kanazawa University, Kakuma-machi, Kanazawa 920-1192, Japan

³Department of Physics, Kyushu University, Hakozaki, Higashi-Ku, Fukuoka 812-8581, Japan

(Received 12 November 2014; accepted 26 December 2014; published online 14 January 2015)

We report real-time detection of hydrogen (H) absorption in metallic palladium (Pd) nano-contacts immersed in liquid H₂ using inelastic electron spectroscopy (IES). After introduction of liquid H₂, the spectra exhibit the time evolution from the pure Pd to the Pd hydride, indicating that H atoms are absorbed in Pd nano-contacts even at the temperature where the thermal process is not expected. The IES time and bias voltage dependences show that H absorption develops by applying bias voltage 30~50 mV, which can be explained by quantum tunneling. The results represent that IES is a powerful method to study the kinetics of high density H on solid surface. © 2015 AIP Publishing LLC. [<http://dx.doi.org/10.1063/1.4905729>]

Hydrogen (H) is ideal replacement for synthetic fuel because of its lightest weight, high abundance, high energy density, and environmental cleanness of the oxidation product. Due to its high chemical reactivity, absorption into metals is a safe way. Moreover, several types of metal compounds can contain H with higher density than liquid H₂ (LH₂).¹ For the industrial applications, elemental processes of H absorption including chemisorption, penetration, and diffusion have been investigated in many metallic systems.²⁻⁴ However, the investigation of H absorption into metal is a challenging issue because of the strong quantum character of H. Actually, quantum phenomena of H, such as quantum tunneling (QT), is reported in metal-hydride and on solid surface.⁴⁻⁹

The kinetics of H on solid surfaces have been investigated with a variety of experiments in ultra-high vacuum environment (e.g., electron diffraction, work function measurements, thermal desorption mass spectrometry, and scanning probe microscopy),^{3,6,10-12} and theoretical calculations.^{3,9,13-15} These results show that H occupation on the surface or subsurface sites is more favorable than that in inner bulk, suggesting that H absorption into bulk is restricted by surface activation barrier at low temperature. On the other hand, some recent experiments suggest that exposure of the surface to high-pressure H₂ urges H penetration into the inside.¹⁶⁻¹⁸ These facts indicate that exploring the interaction between LH₂ or high-density H₂ gas and materials is inevitable to advance H storage technology.

In this Letter, we report the real time detection of H absorption into palladium (Pd) immersed in LH₂ through inelastic electron spectroscopy (IES) measurements for Pd nano-contact. When the contact regime is smaller than the mean free path of conduction electrons, the electrons are transferred through the steep potential drop without energy dissipation in the regime (ballistic electron), and then lose

their energy by scattering with excitations such as phonon as illustrated in Fig. 1(a).¹⁹ This leads to a peak anomaly, corresponding to the state density of the excitation, in the differential conductance (dI/dV) spectra. The “ballistic” electron spectroscopy has been employed for the detection of electron-phonon interaction in metallic nano-contacts,²⁰⁻²² and vibrational modes of a single molecular bridge.²³ In the present study, it is used for the detection of vibrational modes of absorbed H atoms. From the IES time and bias voltage dependences of Pd nano-contacts, we reveal that H absorption develops by applying bias voltage 30–50 mV, which can be understood by QT.

We prepare Pd nano-contacts with a mechanically controllable break junction (MCBJ) technique,¹⁹ thus avoiding surface contamination and oxidation. Pd polycrystalline wire (99.998%, 0.2 mm diameter) is stretched by bending a phosphor-bronze beam with a screw and a piezo element in vacuum at low temperatures. Note that the Pd nano-contact diameter varies from nanometers to micrometers and is kept constant over several hours by preventing thermal input.^{24,25} To introduce LH₂, the MCBJ apparatus is installed in an inner cell having flexible bellows inside the vacuum chamber as shown in Fig. 1(b).²⁶

In Figs. 2(a)–2(f), we show dI/dV spectra and the derivative d^2I/dV^2 spectra, for different Pd nano-contacts, measured as a function of bias voltage using a lock-in technique (1 kHz modulation). The data indicate the efficacy of IES for

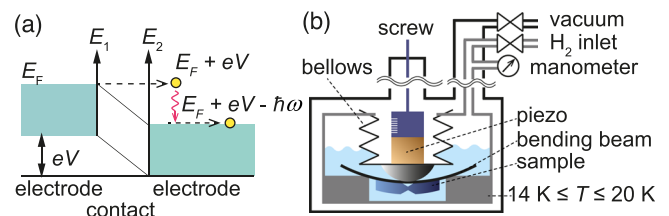


FIG. 1. (a) Energy diagram for ballistic transport of conduction electrons in a Pd nano-contact. (b) Schematic of the MCBJ cryostat. H absorption and diffusion experiments can be carried out in LH₂, avoiding the temperature increase due to Joule heating in the nano-contacts during the measurements.

^{a)}Present address: Institute for Solid State Physics, The University of Tokyo, 5-1-5 Kashiwanoha, Kashiwa-shi, Chiba 277-8581, Japan; Electronic mail: ienaga@issp.u-tokyo.ac.jp

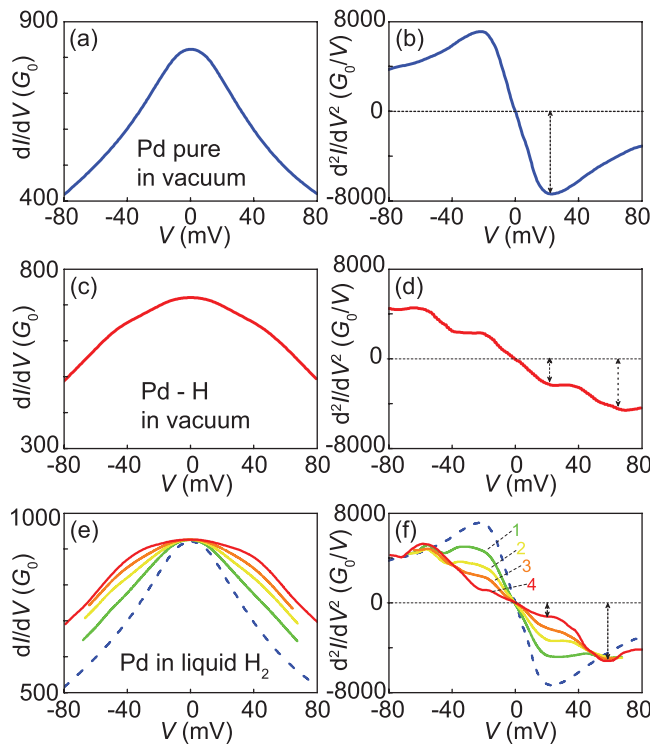


FIG. 2. (a) dI/dV spectrum for a pure Pd nano-contact in vacuum at 18 K, where the vertical axis is the universal conductance unit $G_0 = 2e^2/h$. (b) d^2I/dV^2 spectrum, which is the numerical derivative of (a). (c) dI/dV spectrum of Pd hydride nano-contacts in vacuum at 18 K. (d) d^2I/dV^2 from the dI/dV spectrum of Pd hydride nano-contacts. (e) The time evolution of dI/dV spectra of Pd immersed in LH_2 . For comparison, the spectrum in (a) is plotted in (e) as a dashed line. (f) d^2I/dV^2 spectra of (e). The spectra 1–4 in (e) and (f) are obtained at 500 s, 2500 s, 4500 s, and 8000 s after immersion in LH_2 , respectively.

the detection of H absorption. In the spectra of pure Pd (Figs. 2(a) and 2(b)), the peak in d^2I/dV^2 at $|V| \sim 20$ mV is caused by electron-phonon scattering.^{20–22} The spectra of Pd hydride in vacuum are shown in Figs. 2(c) and 2(d). To prepare Pd hydride, Pd wire is exposed to 1 atm of H_2 gas in the inner cell at 300 K for a few hours, creating a hydrogen concentration of ~ 0.6 .²⁷ Then, the H_2 gas is pumped out of the MCBJ apparatus at 80 K to prevent H desorption from the Pd. The nano-contact is formed by stretching the Pd hydride at 18 K. The spectra in Figs. 2(c) and 2(d) differ from those of pure Pd in that a new peak at $|V| \sim 60$ mV is present and comes from electron scattering with vibrational modes of H atoms in fcc Pd octahedral sites.^{8,23,28}

After preparing the pure Pd nano-contact in vacuum at 18 K, the inner cell is filled by LH_2 . Then, sweep measurements of $|V| \leq 80$ mV are performed repeatedly at 18 K. The dI/dV and d^2I/dV^2 spectra exhibit the time evolution shown in Figs. 2(e) and 2(f). The spectra clearly evolve from pure Pd in Figs. 2(a) and 2(b) to the hydride spectra in Figs. 2(c) and 2(d); the peak at $|V| \sim 20$ mV is suppressed while the new peak at $|V| \sim 60$ mV grows. These demonstrate that H is gradually absorbed by the Pd up to its 18 K limit. Note that the background of electron-phonon interaction superposes on the spectra above $|V| \geq 20$ mV, which covers the growth of the peak at $|V| \sim 60$ mV in Fig. 2(f). The spectrum 3 in Fig. 2(f) is nearly identical to that in Fig. 2(d), indicating that the final H concentration is expected to be higher than ~ 0.6 . Given that superconductivity in the PdH_x systems is

not observed at temperatures above 1.5 K, H concentration must be $x < 0.84$.²⁹

We closely examined the time evolution of the peak amplitude at 20 mV for the Pd nano-contact immersed in LH_2 , because the peak reflecting the electron-phonon interaction is sensitive to the amount of H, as shown in Fig. 2(f) and as discussed later. Moreover, the bias effect is not large at this voltage. In these measurements, the contact diameter is kept 10 nm with feedback adjustment, corresponding to $G(0) \sim 1000 G_0$, where $G(0)$ is the zero-bias conductance obtained from dI/dV at 0 mV. We sweep the bias for $|V| \leq 20$ mV only three times: initially, at 2000 s, then at 40 000 s, after introduction of LH_2 , while keeping $|V| = 0$ mV otherwise. As seen in the spectra of Figs. 3(a) and 3(b), the d^2I/dV^2 amplitude decreases only at 2000 s, with no decrease at 40 000 s.

The amplitude at 20 mV in Fig. 3(b) is much larger than the full absorption at $T = 18$ K in Fig. 2(f), suggesting that the Pd sample has room to absorb more H atoms and that the bias voltage is related to the H absorption. Thus, we examine the bias effect for H absorption by applying a constant bias $V_{\text{const}} = 20$ mV during the measurement for the same sample used in Figs. 3(a) and 3(b). Then, we increase V_{const} to 60 mV in 10 mV steps. The time evolution of the d^2I/dV^2 amplitude at each bias voltage is plotted in Fig. 3(e). At $V_{\text{const}} = 20$ mV, d^2I/dV^2 is almost constant, indicating that further absorption does not occur. However, for $V_{\text{const}} = 30$ mV, 40 mV, and 50 mV, d^2I/dV^2 decreases with time. At $V_{\text{const}} = 60$ mV, d^2I/dV^2 is a constant value that is almost identical to that of

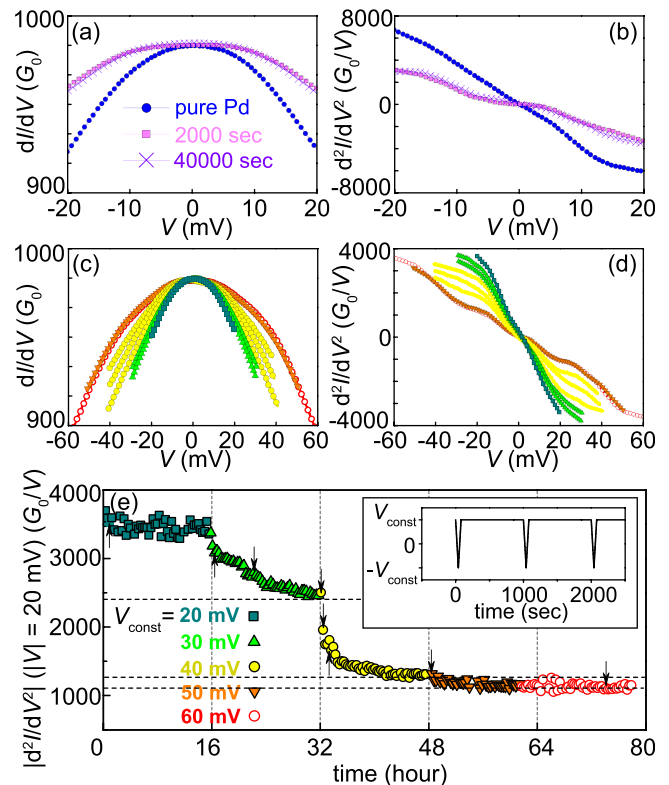


FIG. 3. (a) dI/dV spectra before, at 2000 s, and at 40 000 s after the introduction of LH_2 . (b) d^2I/dV^2 spectra of (a). (c) dI/dV spectra marked by arrows in (e). (d) d^2I/dV^2 spectra of (c). (e) The time and bias dependence of the 20 mV peak height in the spectra, measured by sweeping the bias in $|V| \leq V_{\text{const}}$ every 1000 s, and taken over 16 h at each V_{const} , where the conductance is $1000 G_0$. The inset shows the sequence of the bias sweep.

curve 4 in Fig. 2(f). The amplitudes indicated by arrows in Fig. 3(e) correspond to the spectra in Figs. 3(c) and 3(d). Note that the spectra in Fig. 3(d) evolve similarly as those in Fig. 2(f) do. From these results, it is reasonable to conclude that H absorption occurs because of the applied bias voltage. Moreover, the amount increases monotonically with the bias voltage and saturates at $|V| \sim 60$ mV.

To determine the location of the absorbed H atoms (i.e., on the Pd surface or in the bulk), we investigated the contact-size dependence of d^2I/dV^2 spectra in LH₂, as well as that for pure Pd. The results are plotted in Fig. 4(a) as a function of $G(0)$. The amplitudes at 20 mV in LH₂ are much smaller than those of pure Pd and close to those of Pd hydride at each contact size. In Figs. 4(b) and 4(c), we plot the amplitude at 20 mV and 60 mV as a function of the contact diameter d , estimated from $G(0)$ using the Sharvin relation.³⁰ The amplitudes at 20 mV of pure Pd are proportional to $d^{3.2}$, which is understood in terms of the volume dependence of the acoustic phonon vibration in a pure Pd crystal.³¹ In contrast, the amplitudes at 20 mV of Pd hydride change to $d^{2.4}$ dependence, which indicate that the peak is suppressed with the increase in d . The decrease of the power is probably explained by the suppression of electron-phonon interaction due to H absorption, which is observed in electronic resistivity measurements.³² Since volume/surface ratio increases with increasing d , the ratio of H occupation sites to Pd atoms constructing the contact increases with d . As a result, the power is decreased from 3.2 to 2.4 by H absorption in Pd contact.

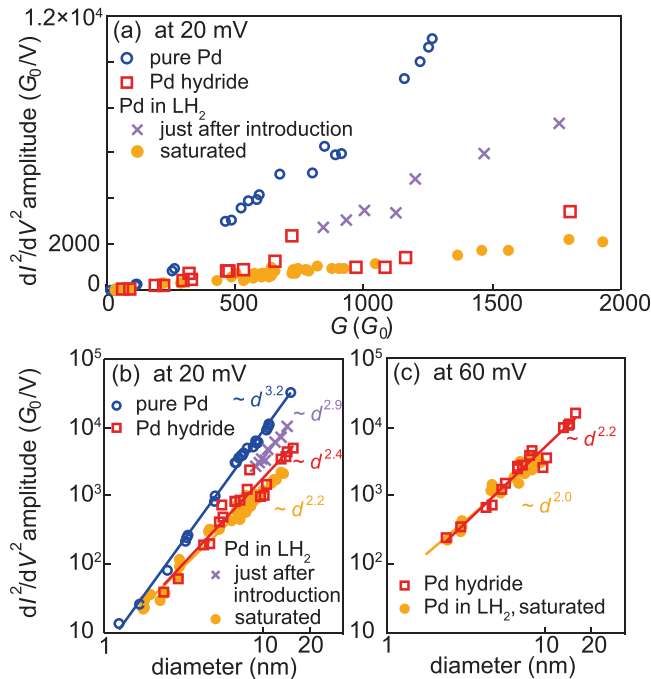


FIG. 4. (a) The amplitude in d^2I/dV^2 at 20 mV for pure Pd nano-contacts (open circle), for Pd hydrides (square), for Pd nano-contacts in LH₂ measured just after the introduction of H₂ (cross), and after the application of the 60 mV bias voltage in Fig. 3(d) (full circle). They are plotted as a function of zero-bias conductance $G(0)$. (b) Plot of the same data in (a) as a function of the diameter d , which is estimated from the conductance. (c) The size dependences of the amplitude in d^2I/dV^2 at 60 mV for Pd hydrides, and Pd nano-contacts in LH₂ after the application of the 60 mV bias voltage in Fig. 3(d). The solid lines are least-squares fits.

In the case of Pd in LH₂, it is important to note that the amplitudes at 20 mV are proportional to $d^{2.9}$ just after introducing the LH₂. After saturation of H absorption, the amplitudes at 20 mV show $d^{2.2}$ dependence, which is close to that of Pd hydride. Moreover, the d -dependences of amplitudes at 60 mV for Pd nano-contacts in LH₂ and Pd hydrides are almost the same as shown in Fig. 4(c). The change of power for Pd nano-contacts by introduction of LH₂ is well explained by the development of H absorption from near-surface region to inner bulk. From these results, we conclude that, after applying the bias voltage, H atoms are absorbed uniformly in the bulk of the Pd contact.

Generally, H absorption in metals occurs in three steps: H chemisorption from dissociated H₂ molecules on the surface, H penetration from the surface, and H diffusion in the bulk. Even at low temperatures, the dissociation of H₂ into H atoms proceeds on the Pd surface spontaneously because of the energy difference between the two states.³ Therefore, H atoms are sufficiently supplied at the Pd surface in LH₂. Moreover, the spectra in Figs. 3(a) and 3(b) change soon after introducing LH₂, and the absorption develops depending on the bias voltage. These results clearly reflect the later two steps, H penetration and H diffusion in the bulk. The rapid change in Figs. 3(a) and 3(b) corresponds to the H penetration from the surface into near-surface region due to high-pressure effects.^{16,17} Taking into account that the H diffusion in bulk is rate-limiting process when H₂ pressure is sufficiently high,¹¹ the time and bias dependences of IES spectra in Figs. 3(c)–3(e) are reasonably understood by H diffusion in bulk Pd.

Thermal hopping and QT are the two possible diffusion modes. In thermal diffusion, H atoms in fcc octahedral Pd sites must acquire the energy to surmount the activation barrier $E_{\text{diff}} \sim 226$ meV.⁸ The diffusion coefficient is given by $D = D_0 \exp(-E_{\text{diff}}/k_B T)$, where $D_0 = 2.9 \times 10^{-7}$ m²/s for Pd and k_B is Boltzmann's constant. At $T = 18$ K, $D \sim 10^{-70}$ m²/s, suggesting that the thermal process is highly unlikely. QT can explain the bias dependence shown in Fig. 3(e) as follows. Because of lattice strain, H atoms undergo the “self-trap effect” in Pd, as illustrated in Fig. 5(a), where they are initially ~ 50 meV lower in energy than corresponding levels in the absence of H atoms.⁷ QT diffusion occurs when an H atom tunnels through the barrier of the potential well trapping the H atom into the well corresponding to absence of H, as shown in Fig. 5(b). This process is assisted by phonons, which raise the energy of the trapped H atoms.^{7,8} Because nano-contacts prepared by MCBJ inevitably have lattice

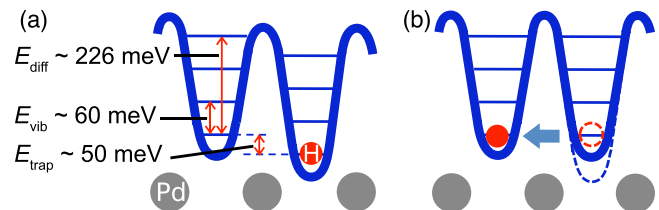


FIG. 5. (a) The self-trapped state of an H atom, where the energy level of the atom is lowered by ~ 50 meV as a result of lattice strain. (b) The diffusion process from the self-trapped state, where the H atom is excited by phonons created by scattered inelastic electrons, and can tunnel to the neighbouring site.

disorders, it is most likely that the bias dependence for the amount of H absorption in Fig. 3(e) is derived from the distribution of potential depths. Moreover, it seems that the spatial distribution changes the relaxation speed, as shown in Fig. 3(e). We estimate that $D \sim 10^{-21} \text{ m}^2/\text{s}$ by the equation, $R_D = \sqrt{D\Delta t}$, where the contact radius R_D and the relaxation time Δt are 5 nm at $\sim 1000 G_0$ and $\sim 10000 \text{ s}$ at $V_{\text{const}} = 40 \text{ mV}$, respectively. This D is considerably larger than that for thermal diffusion at 18 K, as estimated above, indicating that the diffusion is governed by QT.

In summary, we study H atom absorption and diffusion in Pd nano-contacts immersed in liquid H_2 using IES measurements. The IES time and bias voltage dependences demonstrate that H absorption develops by applying the bias voltage 30–50 mV, which can be explained by QT process assisted by phonons induced by ballistic electrons. The present results indicate that QT of atoms can be studied by transport measurements as done in electronic systems, where many characteristic features have been revealed. Moreover, IES is a powerful method to investigate H diffusion in metals exposed to LH_2 or high pressure H_2 .

This work was supported by a Grant-in-Aid for Scientific Research (Grant Nos. 25220605, 25287076, and 26600102) from the Japan Society for the Promotion of Science. K.I. is financially supported by the Japan Society for the Promotion of Science for Young Scientists (Grant No. 12J06024).

¹L. Schlapbach and A. Züttel, *Nature* **414**, 353 (2001).

²A. Pundt and R. Kirchheim, *Annu. Rev. Mater. Res.* **36**, 555 (2006).

³K. Christmann, *Surf. Sci. Rep.* **9**, 1 (1988).

⁴Y. Fukai, *The Metal-Hydrogen System*, 2nd ed. (Springer, Berlin, 2005).

⁵R. R. Arons, Y. Tamminga, and G. de Vries, *Phys. Status Solidi* **40**, 107 (1970).

⁶L. J. Lauhon and W. Ho, *Phys. Rev. Lett.* **85**, 4566 (2000).

⁷C. P. Flynn and A. M. Stoneham, *Phys. Rev. B* **1**, 3966 (1970).

⁸Y. Fukai and H. Sugimoto, *Adv. Phys.* **34**, 263 (1985).

⁹N. Ozawa, N. B. Arboleda, Jr., T. Roman, H. Nakanishi, W. A. Dinão, and H. Kasai, *J. Phys. Condens. Matter* **19**, 365214 (2007).

¹⁰G. E. Gdowski, T. E. Felter, and R. H. Stulen, *Surf. Sci.* **181**, L147 (1987).

¹¹H. Okuyama, W. Siga, N. Takagi, M. Nishijima, and T. Aruga, *Surf. Sci.* **401**, 344 (1998).

¹²E. C. H. Sykes, L. C. Fernández-Torres, S. U. Nanayakkara, B. A. Mantooth, R. M. Nevin, and P. S. Weiss, *Proc. Natl. Acad. Sci. U.S.A.* **102**, 17907 (2005).

¹³P. Ferrin, S. Kandoi, A. U. Nilekara, and M. Mavrikakis, *Surf. Sci.* **606**, 679 (2012).

¹⁴B. Hammer and J. K. Nørskov, *Surf. Sci.* **343**, 211 (1995).

¹⁵O. M. Løvvik and R. A. Olsen, *Phys. Rev. B* **58**, 10890 (1998).

¹⁶S. Ohno, M. Wilde, and K. Fukutani, *J. Chem. Phys.* **140**, 134705 (2014).

¹⁷A. Groß, *Chemphyschem* **11**, 1374 (2010).

¹⁸M. Wilde and K. Fukutani, *Phys. Rev. B* **78**, 115411 (2008).

¹⁹N. Agraït, A. L. Yeyati, and J. M. van Ruitenbeek, *Phys. Rep.* **377**, 81 (2003).

²⁰I. K. Yanson and Yu. N. Shalov, *Sov. Phys. JETP* **44**, 148–155 (1976).

²¹A. G. M. Jansen, F. M. Mueller, and P. Wyder, *Science* **199**, 1037–1040 (1978).

²²Y. G. Naidyuk and I. K. Yanson, *Point-Contact Spectroscopy* (Springer, Berlin, 2004).

²³S. Csonka, A. Halbritter, G. Mihály, O. I. Shklyarevskii, S. Speller, and H. van Kempen, *Phys. Rev. Lett.* **93**, 016802 (2004).

²⁴K. Ienaga, N. Nakashima, Y. Inagaki, H. Tsujii, S. Honda, T. Kimura, and T. Kawae, *Phys. Rev. B* **86**, 064404 (2012).

²⁵K. Ienaga, N. Nakashima, Y. Inagaki, H. Tsujii, T. Kimura, and T. Kawae, *Appl. Phys. Lett.* **101**, 123114 (2012).

²⁶K. Ienaga, T. Yokota, N. Nakashima, Y. Inagaki, H. Tsujii, and T. Kawae, *J. Phys.: Conf. Ser.* **400**, 042019 (2012).

²⁷E. Wicke and H. Brodowsky, *Hydrogen in Metals II*, edited by G. Alefeld and J. Voelkl (Springer, Berlin, 1978).

²⁸J. M. Rowe, J. J. Rush, H. G. Smith, M. Mostoller, and H. E. Flotow, *Phys. Rev. Lett.* **33**, 1297 (1974).

²⁹R. W. Standley, M. Steinback, and C. B. Satterthwaite, *Solid State Commun.* **31**, 801 (1979).

³⁰Y. V. Sharvin, *Sov. Phys. JETP* **21**, 655 (1965).

³¹I. K. Yanson, V. V. Fisun, R. Hesper, A. V. Khotkevich, J. M. Krans, J. A. Mydosh, and J. M. van Ruitenbeek, *Phys. Rev. Lett.* **74**, 302 (1995).

³²H. Akaki, Y. Sakamaki, S. Harada, and M. Kubota, *J. Alloys Compd.* **446**, 436 (2007).